

Differential effects of ocean acidification on carbon acquisition in two bloom-forming dinoflagellate species

Tim Eberlein^{a,*}, Dedmer B. Van de Waal^{a,b} and Björn Rost^a

^aDepartment of Marine Biogeoscience, Alfred Wegener Institute for Polar and Marine Research, Bremerhaven, Germany

^bDepartment of Aquatic Ecology, Netherlands Institute of Ecology (NIOO-KNAW), 6700 AB Wageningen, The Netherlands

Correspondence

*Corresponding author,
e-mail: Tim.Eberlein@awi.de

Received 30 September 2013;
revised 18 November 2013

doi:10.1111/ppl.12137

Dinoflagellates represent a cosmopolitan group of phytoplankton with the ability to form harmful algal blooms. Featuring a Ribulose-1,5-bisphosphate carboxylase/oxygenase (RubisCO) with very low CO₂ affinities, photosynthesis of this group may be particularly prone to carbon limitation and thus benefit from rising atmospheric CO₂ partial pressure (*p*CO₂) under ocean acidification (OA). Here, we investigated the consequences of OA on two bloom-forming dinoflagellate species, the calcareous *Scrippsiella trochoidea* and the toxic *Alexandrium tamarense*. Using dilute batch incubations, we assessed growth characteristics over a range of *p*CO₂ (i.e. 180–1200 µatm). To understand the underlying physiology, several aspects of inorganic carbon acquisition were investigated by membrane-inlet mass spectrometry. Our results show that both species kept growth rates constant over the tested *p*CO₂ range, but we observed a number of species-specific responses. For instance, biomass production and cell size decreased in *S. trochoidea*, while *A. tamarense* was not responsive to OA in these measures. In terms of oxygen fluxes, rates of photosynthesis and respiration remained unaltered in *S. trochoidea* whereas respiration increased in *A. tamarense* under OA. Both species featured efficient carbon concentrating mechanisms (CCMs) with a CO₂-dependent contribution of HCO₃⁻ uptake. In *S. trochoidea*, the CCM was further facilitated by exceptionally high and CO₂-independent carbonic anhydrase activity. Comparing both species, a general trade-off between maximum rates of photosynthesis and respective affinities is indicated. In conclusion, our results demonstrate effective CCMs in both species, yet very different strategies to adjust their carbon acquisition. This regulation in CCMs enables both species to maintain growth over a wide range of ecologically relevant *p*CO₂.

Abbreviations – CA, carbonic anhydrase; CCM, carbon concentrating mechanism; Chl *a*, chlorophyll *a*; C_i, inorganic carbon; CO₃²⁻, carbonate ion; DBS, dextran-bound sulphonamide; DIC, dissolved inorganic carbon; eCA, extracellular carbonic anhydrase; HCO₃⁻, bicarbonate; HEPES, 4-(2-hydroxyethyl)-1-piperazine-ethanesulfonic acid; K_{1/2}, half-saturation concentration; MIMS, membrane-inlet mass spectrometry; OA, ocean acidification; *p*CO₂, atmospheric CO₂ partial pressure; PFD, photon flux density; PIC, particulate inorganic carbon; POC, particulate organic carbon; PON, particulate organic nitrogen; PST, paralytic shellfish poisoning toxins; RubisCO, Ribulose-1,5-bisphosphate carboxylase/oxygenase; TA, total alkalinity.

Introduction

Since the Industrial Revolution, alterations in fossil fuel combustion and land-use have caused atmospheric CO₂ partial pressure (*p*CO₂) to increase from approximately 280 toward approximately 395 μatm at present-day, and is predicted to reach values of approximately 900 μatm by the end of the 21st century (IPCC 2007). Regarding the oceans, elevated *p*CO₂ causes an increase in CO₂ and bicarbonate (HCO₃⁻) concentrations, while carbonate ion concentrations (CO₃²⁻) decrease. These changes in the speciation of dissolved inorganic carbon (DIC) result in lowered pH values, a phenomenon also known as ocean acidification (OA; Wolf-Gladrow et al. 1999, Caldeira and Wickett 2003). OA and associated changes in the carbonate chemistry have been shown to impact marine organisms in many ways (Fabry et al. 2008). Especially for phytoplankton, being the base of the marine food web and the driver of the biological carbon pumps, such changes may have far reaching consequences (Falkowski et al. 1998, Doney et al. 2009).

Phytoplankton take up inorganic carbon and fix CO₂ into organic compounds by Ribulose-1,5-bisphosphate carboxylase/oxygenase (RubisCO). This enzyme generally features low affinities for CO₂, and a competing reaction with O₂ further reduces its overall efficiency (Badger et al. 1998). To overcome these catalytic limitations imposed by RubisCO, phytoplankton developed so-called carbon concentrating mechanisms (CCMs). Common features of a CCM include active uptake of CO₂ and HCO₃⁻ as well as means to reduce the CO₂ leakage (Giordano et al. 2005, Rost et al. 2006). CCMs may further involve carbonic anhydrase (CA), an enzyme which accelerates the otherwise slow interconversion between CO₂ and HCO₃⁻. The mode and cost of CCMs will to a great extent determine the sensitivity of phytoplankton toward OA (Rost et al. 2008, Reinfelder 2011).

The functioning of CCMs has been intensively studied in various phytoplankton species. In diatoms, CCMs were generally downregulated with increasing *p*CO₂ as reflected by lowered photosynthetic affinities for CO₂ and DIC (Burkhardt et al. 2001, Trimborn et al. 2008). Often, these changes were also accompanied by lowered contribution of HCO₃⁻ uptake or decreased activities of extracellular CA (eCA). In other taxa such as the coccolithophore *Emiliania huxleyi* or the cyanobacterium *Trichodesmium*, affinities for CO₂ and DIC were also downregulated under OA, yet eCA activity did not seem to play a role in the functioning of their CCMs (Rost et al. 2003, Kranz et al. 2009). These different modes of CCMs and their regulation with *p*CO₂ have increased our understanding about species-specific responses toward OA in diatoms, coccolithophores and

cyanobacteria. Little is yet known about other taxa, such as dinoflagellates.

Earlier work suggested severe CO₂ limitation in photosynthesis of dinoflagellates (Colman et al. 2002, Dason et al. 2004). This was attributed to their type II RubisCO, which has the lowest affinity for CO₂ of all eukaryotic phytoplankton (Morse et al. 1995, Badger et al. 1998), as well as limited ability to use HCO₃⁻. Recent studies have, however, demonstrated high HCO₃⁻ uptake rates in the dinoflagellate species *Ceratium lineatum*, *Heterocapsa triquetra*, *Prorocentrum minimum* (Rost et al. 2006, Fu et al. 2008) and *Protoceratium reticulatum* (Ratti and Giordano 2007), indicating rather efficient modes of CCMs that may make them relatively independent from changes in CO₂ availability. In some dinoflagellates, CCMs have been shown to respond to changes in carbonate chemistry, e.g. by lowered photosynthetic affinities for CO₂ and DIC (Rost et al. 2006, Ratti and Giordano 2007), or by downregulation of CA transcripts (Van de Waal et al. 2013) with increasing *p*CO₂. Such apparent differences in the regulation of CCMs may explain the observed variability in responses to OA in growth and primary production of different dinoflagellate species (Fu et al. 2007, 2010) or strains (Brading et al. 2011, 2013).

To improve our understanding about growth responses and the functioning of CCMs in dinoflagellates under OA, this study investigated the eco-physiology of two distinct dinoflagellate species, the calcareous *Scrippsiella trochoidea* and the toxic *Alexandrium tamarense* over a range of *p*CO₂. Both are bloom-forming species that co-occur in the North Sea (Fistarol et al. 2004, McCollin et al. 2011). As one has the potential to calcify and the other is a potent toxin producer, different ecological strategies can be expected, which may also be reflected in the functioning of their CCM. Hence, measurements on growth and biomass production were accompanied by measurements on inorganic carbon fluxes and CA activities using membrane-inlet mass spectrometry (MIMS).

Materials and methods

Species and growth conditions

Scrippsiella trochoidea Geob267 (culture collection of the University of Bremen) and *Alexandrium tamarense* Alex5 (Tillmann et al. 2009), both isolates from the North Sea, were cultured at 15°C in 0.2 μm filtered North Sea water (salinity 34). Vitamins and trace metals were added according to *f/2* medium (Guillard and Ryther 1962), except for FeCl₃ (1.9 μmol l⁻¹), H₂SeO₃ (10 nmol l⁻¹) and NiCl₂ (6.3 nmol l⁻¹). Nitrate and

phosphate were added to final concentrations of 100 and 6.25 $\mu\text{mol l}^{-1}$, respectively. Culture medium was pre-aerated with air containing $p\text{CO}_2$ of 180 μatm (Last Glacial Maximum), 380 μatm (present-day), 800 μatm and 1200 μatm (scenarios of the year 2100 and beyond). These concentrations were obtained by mixing CO_2 -free air ($<0.1 \mu\text{atm } p\text{CO}_2$; Domnick Hunter, Willich, Germany) with pure CO_2 (Air Liquide Deutschland, Düsseldorf, Germany) using mass flow controllers (CGM 2000 MCZ Umwelttechnik, Bad Nauheim, Germany). CO_2 concentrations were regularly verified by a non-dispersive infrared analyzer system (LI6252, LI-COR Biosciences, Bad Homburg, Germany).

Cultures were grown in 2.4 l borosilicate bottles and placed on a roller table to allow homogenous mixing. Light was provided by OSRAM daylight tubes (18 W/965 Biolux) at a light:dark cycle of 16:8 h. Light was adjusted to an incident photon flux density (PFD) of $250 \pm 25 \mu\text{mol photons m}^{-2} \text{s}^{-1}$ using a spherical micro quantum sensor (Walz, Effeltrich, Germany). Prior to the onset of the experiments, cells were acclimated to the respective CO_2 concentrations for at least 14 days. To ensure dilute batch conditions with minor changes in carbonate chemistry, cultures were diluted about once a week and population densities were kept $<400 \text{ cells ml}^{-1}$. Experiments were run in triplicates ($n = 3$) over at least 5 days.

Sampling and analyses

Samples were always taken 5–7 h after the start of the light period. Every other day, pH was measured with a 2-point calibrated WTW pH meter 3110 (Wissenschaftlich-Technische Werkstätten GmbH, Weilheim, Germany). Samples for total alkalinity (TA) were analyzed by a fully automated titration system (SI Analytics, Mainz, Germany) with a mean accuracy of $13 \mu\text{mol l}^{-1}$. DIC samples were analyzed in a QuAatro high performance microflow analyzer (Seal, Mequon, WI) with a mean accuracy of $8 \mu\text{mol l}^{-1}$. Changes in TA and DIC over the course of the incubations were <2 and $<3.4\%$, respectively. Owing to the decreasing buffer capacity with increasing $p\text{CO}_2$ (Egleston et al. 2010), DIC consumption caused higher variability in pH and $p\text{CO}_2$ in the high CO_2 treatments (Table 1). Carbonate chemistry was calculated with CO2sys (Pierrot et al. 2006) using pH_{NBS} (National Bureau of Standards) and TA of each incubation. Equilibrium constants of Mehrbach et al. (1973), refitted by Dickson and Millero (1987) were chosen.

To determine population densities, 20–60 ml culture suspension was fixed with Lugol's solution (2% final concentration). Each day, triplicate cell counts were

Table 1. Carbonate chemistry for the different CO_2 treatments. Values for TA, DIC and pH indicate the mean of triplicate incubations ($n = 3$; $\pm \text{SD}$). $p\text{CO}_2$ was calculated based on pH and TA of each incubation, using equilibrium constants by Mehrbach et al. (1973), refitted by Dickson and Millero (1987).

CO_2 treatment	TA ($\mu\text{mol l}^{-1}$)	DIC ($\mu\text{mol l}^{-1}$)	pH_{NBS}	$p\text{CO}_2$ (μatm)
<i>S. trochoidea</i>				
180	2386 ± 1	1972 ± 16	8.45 ± 0.01	180 ± 6
380	2388 ± 2	2096 ± 10	8.21 ± 0.02	358 ± 15
800	2385 ± 1	2223 ± 11	7.91 ± 0.03	785 ± 55
1200	2386 ± 4	2268 ± 18	7.77 ± 0.04	1133 ± 97
<i>A. tamareuse</i>				
180	2434 ± 3	1992 ± 33	8.50 ± 0.06	162 ± 24
380	2439 ± 1	2117 ± 41	8.27 ± 0.07	315 ± 57
800	2434 ± 2	2245 ± 37	7.97 ± 0.10	706 ± 154
1200	2418 ± 1	2283 ± 34	7.83 ± 0.12	995 ± 248

performed with an Axiovert 40C inverted microscope (Carl Zeiss MicroImaging GmbH, Hamburg, Germany). Specific growth rates (μ) were calculated by an exponential fit through cell counts over at least 4 days for each biological replicate ($n = 3$).

At the end of each experiment, samples were taken to assess particulate organic carbon and nitrogen (POC and PON), particulate inorganic carbon (PIC, as difference between total particulate carbon and POC), as well as chlorophyll *a* (Chl *a*). For analyses of POC and PON, 300–400 ml culture suspension was filtered in duplicate on pre-combusted GF/F filters (500°C , 6 h). Prior to POC measurements, 200 ml of HCl (0.1 mol l^{-1}) was added to the filters to remove all PIC, and filters were dried overnight. Filters were wrapped in tin foil cups and analyzed by an ANCA-SL 20–20 mass spectrometer (SerCon Ltd., Crewe, UK). To determine Chl *a*, 100–200 ml culture suspension was filtered in duplicate on cellulose-nitrate filters (Whatman, Maidstone, UK), rapidly frozen in liquid nitrogen and subsequently stored at -80°C . Extraction and fluorometric determination of Chl *a* were done according to Knap et al. (1996), using a TD-700 Fluorometer (Turner Designs, Sunnyvale, CA).

Oxygen and inorganic carbon flux measurements

O_2 and CO_2 fluxes were measured by means of MIMS (Isoprime, GV Instruments, Manchester, UK) to determine photosynthetic O_2 evolution and respiratory O_2 uptake, as well as CO_2 and HCO_3^- fluxes. Net O_2 fluxes were converted to inorganic carbon (C_i) fluxes by applying a photosynthetic quotient of 1.4 (as nitrate was the only nitrogen source in the growth medium) and a respiratory quotient of 1.0 (Williams and Robertson 1991). The applied approach by Badger et al. (1994) depends on a chemical disequilibrium between CO_2

and HCO_3^- , which is induced by photosynthetic C_i uptake in the absence of eCA activity. O_2 and CO_2 fluxes were measured simultaneously during steady-state photosynthesis in consecutive light–dark intervals with increasing amounts of DIC. Maximum rates (V_{max}) and half-saturation concentrations ($K_{1/2}$) for respective C_i species (CO_2 and HCO_3^-) and DIC were determined by applying a Michaelis–Menten fit. Negative estimates of HCO_3^- concentrations, which were occasionally calculated for the lowest DIC concentrations, were omitted from the Michaelis–Menten fit. Measurements were performed in a 4-(2-hydroxyethyl)-1-piperazine-ethanesulfonic acid (HEPES, 50 mmol l^{-1}) buffer in f/2 medium with a pH of 8.0 ± 0.1 at $15 \pm 0.3^\circ\text{C}$. The applied pH in the MIMS assay represents an intermediate value of the pH values of the acclimations. Provided that these differences in pH have minor effects on C_i uptake kinetics, rates in the assays are also representative for the acclimation. For more details on the method see Badger et al. (1994) and Rost et al. (2007).

Prior to the experimental series, the shape and speed of the stirrer in the MIMS-cuvette were tested on both species to eliminate biases from mechanical and physiological stress for the dinoflagellate species. In test runs, photosynthetic O_2 and respiration evolution was measured in intervals for about 1 h, confirming that rates remained unaffected over the duration of the assay. Light and dark intervals were adjusted to 4.5 and 3.5 min, respectively, to allow the CO_2 and O_2 traces to reach steady-state conditions (i.e. a linear slope; see Rost et al. 2006). The light intensity in the cuvette was set to the light intensity of the experiments (tested with the same light meter) with very comparable light spectra as similar daylight tubes have been used. Prior to the measurements, acclimated dinoflagellate cells were concentrated by gentle vacuum filtration ($<200 \text{ mbar}$) over a $10 \mu\text{m}$ membrane filter (Millipore, Billerica, MA). Culture medium was exchanged with DIC-free assay medium and 8 ml of this concentrated cell suspension was transferred into the MIMS cuvette. During the first dark phase, membrane-impermeable dextran-bound sulphonamide (DBS; Synthelec AB, Lund, Sweden) was added to a final concentration of $50 \mu\text{mol}$ to inhibit any potential eCA activity. In order to normalize rates, duplicate Chl *a* samples were taken after each measurement.

Extracellular carbonic anhydrase activities

The determination of eCA activity was monitored by the ^{18}O depletion rate of doubly labeled $^{13}\text{C}^{18}\text{O}_2$ in sea water via alternating hydration and dehydration steps (Silverman 1982). As CA catalyzes the interconversion

between HCO_3^- and CO_2 , it concomitantly enhances the exchange of ^{18}O in $^{13}\text{C}^{18}\text{O}^{18}\text{O}$ ($m/z = 49$) with ^{16}O from water molecules, forming $^{13}\text{C}^{18}\text{O}^{16}\text{O}$ ($m/z = 47$) and subsequently $^{13}\text{C}^{16}\text{O}^{16}\text{O}$ ($m/z = 45$). In the dark, $\text{NaH}^{13}\text{C}^{18}\text{O}_3$ label was injected into the cuvette containing 8 ml HEPES-buffered culture medium with a pH of 8.0 ± 0.1 at $15 \pm 0.3^\circ\text{C}$. After recording the steady-state depletion in ^{18}O enrichment for approximately 8 min (S_1), $400 \mu\text{l}$ of the concentrated cell suspension was injected, and the ^{18}O depletion was followed for another 10 min (S_2). Units of eCA activity (U) were calculated using the catalyzed and non-catalyzed rates S_2 and S_1 , respectively, and subsequently normalized to Chl *a* (Badger and Price 1989). As a consequence, U corresponds to the enhancement in the interconversion between CO_2 and HCO_3^- , expressed as $\% \mu\text{g Chl } a^{-1}$. For more details on the method see Palmqvist et al. (1994) and Rost et al. (2007).

Statistics

Normality of data was confirmed using the Shapiro-Wilk test. Variables were log-transformed if this improved the homogeneity of variances, as tested by Levene's test. Significant differences between treatments were tested using one way ANOVA, followed by post hoc comparison of the means using Tukey's HSD ($\alpha = 0.05$; Quinn and Keough 2002); significant differences between species, i.e. comparing the respective treatments, were tested using *t*-test; significances of relationships between HCO_3^- to net C fixation and CO_2 concentrations were tested by means of linear regression.

Results

Growth characteristics

In both species, growth remained largely unaffected by changes in $p\text{CO}_2$ (Table 2), but *S. trochoidea* grew significantly faster than *A. tamarensis* ($P < 0.001$) with average growth rates of $0.60 \pm 0.05 \text{ day}^{-1}$ compared to $0.47 \pm 0.02 \text{ day}^{-1}$, respectively. *Scrippsiella trochoidea* displayed a decrease in POC quota in response to elevated $p\text{CO}_2$ (Table 2), which was in line with a reduction in cell size (data not shown). In *A. tamarensis*, POC quota remained unaltered over the applied $p\text{CO}_2$ range (Table 2), and were about twofold higher compared to *S. trochoidea*. Chl *a* quota in *S. trochoidea* showed maximum values in the 380 and 800 $\mu\text{atm CO}_2$ treatments, whereas in *A. tamarensis*, they remained largely constant over the $p\text{CO}_2$ range (Table 2). Average Chl *a* quota were about sixfold higher in *A. tamarensis* as compared to *S. trochoidea*. As a consequence of the

Table 2. Growth characteristics of *Scrippsiella trochoidea* and *Alexandrium tamarense* in the different CO₂ treatments. A significant difference between treatments is denoted by different letters. Values represent the mean ± SD of triplicate incubations (n = 3).

pCO ₂ (µatm)	Growth rate (day ⁻¹)	POC production (ng cell ⁻¹ day ⁻¹)	POC production (pg (pg Chl a) ⁻¹ day)	Chl a (pg cell ⁻¹)	POC (ng cell ⁻¹)	POC:PON (molar)	POC:Chl a (mass)
<i>S. trochoidea</i>							
180	0.61 ± 0.03	1.21 ± 0.04 ^a	283 ± 38 ^a	4.3 ± 0.71 ^a	1.99 ± 0.04 ^a	7.6 ± 0.2 ^{ac}	469 ± 81 ^a
380	0.61 ± 0.05	1.08 ± 0.08 ^{ab}	143 ± 13 ^b	7.6 ± 1.19 ^{ab}	1.76 ± 0.02 ^{ab}	8.1 ± 0.3 ^{ab}	236 ± 42 ^b
800	0.61 ± 0.04	1.10 ± 1.14 ^a	127 ± 20 ^b	8.7 ± 0.52 ^b	1.79 ± 0.22 ^{ab}	8.4 ± 0.3 ^b	206 ± 28 ^b
1200	0.58 ± 0.02	0.87 ± 0.02 ^b	188 ± 52 ^b	4.9 ± 1.25 ^a	1.50 ± 0.09 ^b	7.4 ± 0.1 ^c	321 ± 77 ^{ab}
<i>A. tamarense</i>							
180	0.46 ± 0.02 ^{ab}	1.47 ± 0.08	40.5 ± 3.9	36.3 ± 1.52	3.17 ± 0.25	5.8 ± 0.1	88 ± 11
380	0.46 ± 0.02 ^{ab}	1.68 ± 0.12	42.0 ± 4.6	40.1 ± 2.75	3.62 ± 0.31	5.8 ± 0.3	91 ± 9
800	0.48 ± 0.01 ^a	1.67 ± 0.06	42.4 ± 3.1	39.5 ± 3.34	3.46 ± 0.15	5.7 ± 0.1	88 ± 6
1200	0.45 ± 0.01 ^b	1.55 ± 0.06	43.2 ± 7.7	36.4 ± 5.82	3.46 ± 0.17	5.6 ± 0.1	97 ± 15

differences in growth and POC quota, POC production rates of *S. trochoidea* decreased from 180 to 1200 µatm pCO₂ ($P=0.005$; Table 2). *Alexandrium tamarense* displayed no changes in POC production rates toward elevated pCO₂ (Table 2), which were on average twice as high as in *S. trochoidea*.

The POC:PON ratio of *S. trochoidea* ranged between 7.4 and 8.4 with highest values in the 380 and 800 µatm CO₂ treatments, whereas the POC:Chl *a* ratio were highest in the 180 and 1200 µatm CO₂ treatments with 469 ± 81 and 321 ± 77, respectively (Table 2). In *A. tamarense*, POC:PON and POC:Chl *a* ratios remained unaffected by elevated pCO₂ with average values of 5.7 ± 0.2 and 90 ± 10, respectively. Calcification in *S. trochoidea* was very low with PIC:POC ratios <0.1 in all CO₂ treatments (data not shown), suggesting that calcite cyst formation in exponentially growing cells remains low (Wang et al. 2007).

Oxygen and carbon fluxes

In *S. trochoidea*, net photosynthesis (V_{max}) and dark respiration remained largely unaltered between the different CO₂ treatments (Fig. 1). With mean values of 323 ± 68 and 173 ± 21 µmol O₂ (mg Chl *a*)⁻¹ h⁻¹, respectively, net photosynthetic rates were about twofold higher than dark respiration rates. In *A. tamarense*, net photosynthetic rates decreased from 142 ± 4 to 86 ± 11 µmol O₂ (mg Chl *a*)⁻¹ h⁻¹ ($P=0.034$), while dark respiration rates increased from 88 ± 5 to 116 ± 9 µmol O₂ (mg Chl *a*)⁻¹ h⁻¹ from the lowest to the highest CO₂ treatment ($P=0.009$).

Scrippsiella trochoidea preferentially took up HCO₃⁻ with high affinities [i.e. low $K_{1/2}$ (HCO₃⁻); Table 3]. In contrast, *A. tamarense* exhibited a high CO₂ uptake with high affinities [i.e. low $K_{1/2}$ (CO₂); Table 3]. Hence, the relative contribution of CO₂ and HCO₃⁻ to net C fixation differed between the investigated species and

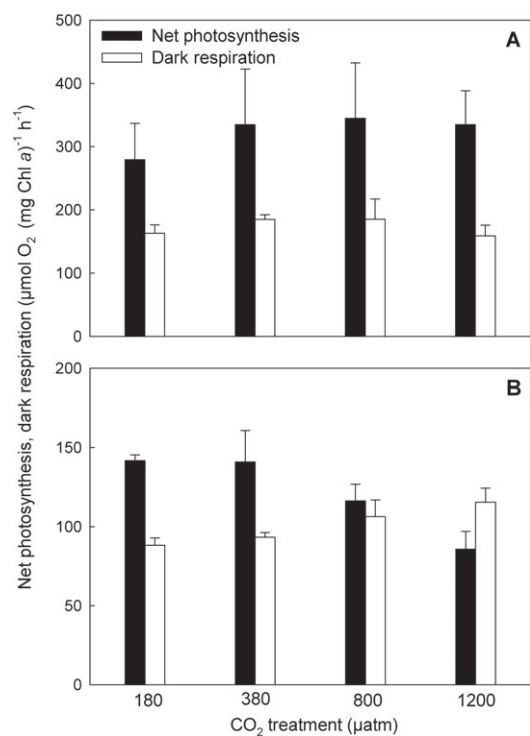


Fig. 1. Chl *a*-specific rates of net photosynthesis and dark respiration of *Scrippsiella trochoidea* (A) and *Alexandrium tamarense* (B) acclimated to different CO₂ concentrations. Bars represent mean ± SD (n = 3).

furthermore changed under elevated pCO₂. *Scrippsiella trochoidea* showed a decrease in the HCO₃⁻ to net C fixation ratio from 0.99 ± 0.17 at the lowest to 0.70 ± 0.14 at the highest CO₂ treatment ($f=1.065 - 0.0009x$; $R^2=0.48$; $P=0.0128$; Fig. 2). *Alexandrium tamarense* used both HCO₃⁻ and CO₂ as carbon source, with an increase in the HCO₃⁻ to net C fixation ratio from 0.36 ± 0.06 at the lowest to 0.64 ± 0.27 at the highest CO₂ treatment ($f=0.29 + 0.0003x$; $R^2=0.40$; $P=0.0280$; Fig. 2).

Table 3. Net C fixation, net CO₂ uptake, HCO₃⁻ uptake, eCA activity and leakage of *Scrippsiella trochoidea* and *Alexandrium tamarense* in the different CO₂ treatments. Values for V_{max} and K_{1/2} are given in μmol mg⁻¹ Chl a h⁻¹ and μmol l⁻¹, respectively. A dash indicates that values could not be determined. If not stated otherwise, values represent the mean ± SD of triplicate incubations (n = 3). A significant difference between treatments is denoted by different letters.

pCO ₂ (μatm)	Net C fixation			Net CO ₂ uptake		HCO ₃ ⁻ uptake		eCA activity U (μg Chl a) ⁻¹	Leakage CO ₂ efflux: total C _i uptake
	V _{max}	K _{1/2} (CO ₂)	K _{1/2} (DIC)	V _{max}	K _{1/2} (CO ₂)	V _{max}	K _{1/2} (HCO ₃ ⁻)		
<i>S. trochoidea</i>									
180	199 ± 41	3.8 ± 0.5	94 ± 50	-13 ± 37 ^a	-	194 ± 5	7.2 ± 12.4	1573 ± 108	0.56 ± 0.06
380	239 ± 62	4.7 ± 1.1	160 ± 40	-7 ± 29 ^a	-	225 ± 40	17 ± 1.4	1416 ± 22	0.53 ± 0.06
800	246 ± 62	5.5 ± 0.9	263 ± 51	-3 ± 40 ^{ab}	-	202 ± 32	3.7 ± 5.5	1232 ± 144	0.54 ± 0.01
1200	239 ± 38	5.1 ± 0.4	269 ± 78	89 ± 22 ^b	20.1 ± 0.6	165 ± 26	10.3 ± 17	1301 ± 99	0.48 ± 0.04
<i>A. tamarense</i>									
180	101 ± 2 ^a	2.4 ± 0.1	267 ± 43	66 ± 9 ^a	3.3 ± 0.2	36 ± 5	105 ± 45	19 ± 48 (n = 2)	0.44 ± 0.01 ^a
380	101 ± 14 ^{ab}	2.8 ± 0.2	309 ± 67	60 ± 16 ^{ab}	3.3 ± 0.3	38 ± 7	220 ± 96	86 ± 2 (n = 2)	0.46 ± 0.02 ^a
800	83 ± 7 ^{ab}	2.0 ± 0.9	206 ± 65	42 ± 8 ^{ab}	3.1 ± 1.0	42 ± 10	158 ± 143	156 ± 12 (n = 2)	0.53 ± 0.02 ^b
1200	61 ± 8 ^c	2.5 ± 0.2	173 ± 15	23 ± 26 ^b	4.5 ± 0.8	38 ± 13	148 ± 28	124 (n = 1)	0.63 ± 0.05 ^c

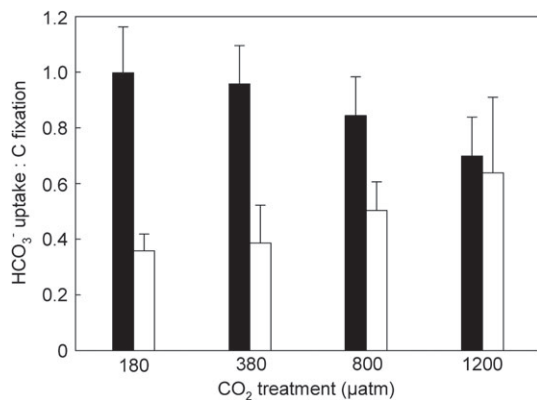


Fig. 2. Contribution of HCO₃⁻ uptake relative to net C fixation of *Scrippsiella trochoidea* (black bars) and *Alexandrium tamarense* (white bars) acclimated to different CO₂ concentrations. Ratios were calculated using the Michaelis–Menten kinetics (Table 3) and the corresponding carbonate chemistry of the respective CO₂ treatments (Table 1). Bars represent mean ± SD (n = 3).

Carbonic anhydrase activity

Scrippsiella trochoidea displayed exceptionally high eCA activities with up to 1600 U (μg Chl a)⁻¹ irrespective of the CO₂ treatments (Table 3). In contrast, *A. tamarense* contained relatively low eCA activities with mean values of 95 U (μg Chl a)⁻¹.

Discussion

In this study, two bloom-forming dinoflagellate species with different traits, the calcifying *S. trochoidea* and the toxic *A. tamarense*, were exposed to a range of pCO₂ to investigate the effects of OA. While growth rates remained largely unaltered, elemental composition and production rates were responsive to OA. Both species

also strongly regulated their underlying physiology with surprisingly different strategies to deal with changes in CO₂ supply.

Growth and biomass production

Both species showed relatively small effects in terms of growth rates, yet we observed CO₂-dependent differences in POC production rates between species. In *S. trochoidea*, POC production rates decreased by almost 30%, which is reflected by a reduced cell size (data not shown) as well as lowered POC quota under elevated pCO₂ (Table 2). On the contrary, in *A. tamarense*, POC production rates and POC quotas remained largely unaltered (Table 2), the latter being similar to Leong et al. (2010). Average Chl a quota in *S. trochoidea* was largely comparable with earlier findings (Haardt and Maske 1987), whereas for *A. tamarense*, the average Chl a quota was about twice as high as earlier reported values (Carreto et al. 2001, Hu et al. 2006). Note that in none of the mentioned studies carbonate chemistry was controlled.

Regarding elemental composition, *S. trochoidea* showed highest POC:PON ratios under intermediate CO₂ concentrations (Table 2), with average ratios being lower than previously observed (approximately 9.3 in Burkhardt et al. 1999). These changes in POC:PON ratios are the result of disproportionately decreasing POC and PON quota under elevated pCO₂. In *A. tamarense*, POC:PON ratios were unaltered by the applied CO₂ treatments, and values were comparable with results of Leong et al. (2010). The significantly lower POC:PON ratio of *A. tamarense*, compared to *S. trochoidea*, may partly be attributed to the fact that it produces nitrogen-rich paralytic shellfish poisoning toxins (PST; Bates et al. 1978). However, the overall contribution of PST to

total cellular nitrogen for this strain of *A. tamarensis* accounts for less than 4% (Van de Waal et al. 2014), and thus cannot alone explain the observed differences in POC:PON between both species.

In contrast to our expectations, processes like growth and elemental ratios were not strongly affected by OA. With respect to POC production, however, species differed in their responses, which could be attributed to CO₂-dependent changes in photosynthesis, in particular in their mode of C_i acquisition. We therefore performed MIMS measurements targeting those underlying processes.

Photosynthesis and respiration

In *S. trochoidea*, rates of O₂ evolution (i.e. net photosynthesis) were more than twofold higher than in *A. tamarensis*, which is in line with higher growth rates as well as higher POC:Chl *a* ratios (Table 2). Both species exhibited high dark respiration rates compared to net photosynthetic rates (Fig. 1). Provided that measured respiration during darkness is representative also for the light phase, respiration was approximately 50% of net photosynthesis in *S. trochoidea*, whereas in *A. tamarensis* both rates were equally high. Comparable high dark respiration rates have since long also been shown for other dinoflagellate species, including zooxanthellae (e.g. Burris 1977). In *A. tamarensis*, net photosynthesis and respiration furthermore showed opposing trends in response to elevated *p*CO₂. The decrease in net photosynthesis in *A. tamarensis* may be largely caused by the increased dark respiration under elevated *p*CO₂. Other processes affecting O₂ uptake in the light, such as Mehler Reaction and photorespiration, can however not be excluded here and may potentially alter the trends. Brading et al. (2013), for example, observed significant light-dependent O₂ uptake in four *Symbiodinium* strains, which remained unaltered under OA. Other studies showed that OA effects can be modulated under different light levels and may enhance mitochondrial respiration, photorespiration and ultimately reduce growth and biomass production under high light (Gao et al. 2012, Rokitta and Rost 2012, Li and Campbell 2013). Interestingly, the increase in respiration with *p*CO₂ observed in *A. tamarensis* was found to have no effect on growth or POC production rates. Overall, it can be concluded that the sum of net photosynthesis and respiration, i.e. gross photosynthesis, remained largely unaffected in both tested species.

Previous studies on *Protoceratium reticulatum* and four strains of *Symbiodinium* showed basically no CO₂ effect on photosynthesis and respiration (Ratti and Giordano 2007, Brading et al. 2011), with the exception

of one *Symbiodinium* strain that showed higher rates of net photosynthesis under OA (Brading et al. 2011). Interestingly, in *Protoceratium reticulatum* and another *Symbiodinium* strain, growth nonetheless increased with elevated *p*CO₂ (Ratti and Giordano 2007, Brading et al. 2011). These findings, together with our current results, demonstrate that responses in growth and biomass production toward OA cannot always be explained by changes in O₂ fluxes, but instead may be attributed to the mode of C_i acquisition. High sensitivities in growth and biomass production toward OA, for instance, have often been associated with a strong dependency on CO₂ as a C_i source for photosynthesis (Colman et al. 2002, Fu et al. 2008), whereas when HCO₃⁻ is the dominant C_i source, much less sensitivity toward changes in CO₂ is expected (Burkhardt et al. 1999, Rost et al. 2008). Therefore, we assessed various key components of the CCM and their potential CO₂-dependent regulation to understand the responses of *S. trochoidea* and *A. tamarensis* toward OA.

Carbon source and carbonic anhydrase

Among the various studies on carbon acquisition in dinoflagellates, either CO₂ (Colman et al. 2002, Dason et al. 2004, Fu et al. 2008, Lapointe et al. 2008, Brading et al. 2013) or HCO₃⁻ (Rost et al. 2006, Ratti and Giordano 2007, Fu et al. 2008) was estimated to be the dominant C_i source. Here we show that *S. trochoidea* and *A. tamarensis* used CO₂ as well as HCO₃⁻ for photosynthesis, though their contribution to net C fixation and response to elevated *p*CO₂ were very different. As one would expect, *S. trochoidea* displayed an increase in relative CO₂ uptake, or in other words, a decrease in relative HCO₃⁻ uptake to net fixation under elevated *p*CO₂ (Fig. 2). Such a trend has also been observed in other functional groups, e.g. diatoms (Burkhardt et al. 2001, Trimborn et al. 2009, 2013), coccolithophores (Rost et al. 2003) or cyanobacteria (Kranz et al. 2009). The response in *A. tamarensis*, however, was surprising as it showed the reverse trend, i.e. an increase of HCO₃⁻ uptake in response to elevated *p*CO₂ (Fig. 2). This could be associated with the generally high and increasing rates of respiration and CO₂ efflux observed in this species (Fig. 1, Table 3). HCO₃⁻ uptake may therefore be simply upregulated to compensate for the increasing CO₂ efflux. Even though respiration can partly cause the high loss of C_i from the cell, it could be speculated that the increase in respiration may also provide the required ATP to fuel the higher HCO₃⁻ uptake. Why mitochondrial activity, in the first place, is stimulated under OA scenarios remains elusive, but it could be associated to altered proton gradients across the mitochondrial membrane or to pH-dependent

changes in the functioning of respiratory enzymes (Amthor 1991).

According to the common notion, eCA functions to replenish the CO₂ pool in the CO₂ depleted boundary layer of a cell, thereby fuelling the CO₂ uptake systems (Badger and Price 1989, Sültemeyer 1998, Elzenga et al. 2000). Such mechanism would obviously be most effective when a cell predominantly uses CO₂ as its C_i source. For dinoflagellates, a major role of eCA activity in CCM functioning was only indicated for the CO₂ user *Lingulodinium polyedrum* and *Symbiodinium* A20 (Lapointe et al. 2008, Brading et al. 2013). Activities of eCA in most other tested dinoflagellates, including *A. tamarense* in this study, were close to detection limits and therefore likely play only a minor role, if any, in C_i acquisition (Table 3; Colman et al. 2002, Rost et al. 2006, Ratti and Giordano 2007). In *S. trochoidea*, however, we observed exceptionally high eCA activities of up to 1600 U (µg Chl a)⁻¹ over the entire pCO₂ range (Table 3). Why would a predominant HCO₃⁻ user have such high eCA activities? Comparable high eCA activities in concert with high HCO₃⁻ contribution have been observed previously (Martin and Tortell 2008, Trimborn et al. 2008, 2013), and our observation that eCA and HCO₃⁻ uptake are both upregulated at high pH casts further doubts on an universal role of eCA.

Trimborn et al. (2008) proposed that in HCO₃⁻ users, eCA may convert effluxing CO₂ to HCO₃⁻, which is subsequently taken up again by the cell. Such a 'CO₂ recycling mechanism' would be particularly advantageous for species with high respiration rates, which was indeed the case for *S. trochoidea* (Fig. 1). For *Thalassiosira* spp., however, the effectiveness of such a mechanism was recently questioned as it would increase the C_i uptake rate by less than 1% only (Hopkinson et al. 2013). This situation may, however, strongly differ between species as model estimates depend on the net CO₂ uptake, which is large for *Thalassiosira* spp. (Hopkinson et al. 2013) but not for *S. trochoidea* (Table 3). In fact, net CO₂ uptake in *S. trochoidea* was close to zero or even negative and there was a high leakage, i.e. about 50% of the C_i taken up by the cell was leaking out as CO₂ (Table 3), which is not accounted for in the model calculations (Hopkinson et al. 2013). Particular high leakage has also been measured in other dinoflagellates (Rost et al. 2006). It should be noted, however, that C_i fluxes are typically determined using disequilibrium approaches and thus require the inhibition of potential eCA activity (Badger et al. 1994). If eCA activity would indeed be involved in minimizing the CO₂ efflux, this approach may overestimate leakage for *S. trochoidea*, while estimates in *A. tamarense*, which lacks eCA activity, would not be biased by the approach.

In any case, although eCA presumably contributes to the CCM, its role and correlation with high HCO₃⁻ uptake remains puzzling and requires further investigations.

CCMs and trade-offs within

With respect to net C fixation, both *S. trochoidea* and *A. tamarense* displayed half-saturation concentrations (K_{1/2}) of <6 µmol CO₂ l⁻¹ at all applied CO₂ levels (Table 3). These results were consistent with previously published K_{1/2} values of other dinoflagellates (Rost et al. 2006, Ratti and Giordano 2007) and fall in the same range as those measured for temperate diatoms (Burkhardt et al. 2001, Trimborn et al. 2008, 2009, Yang and Gao 2012), which are known to feature very effective CCMs (Reinfelder 2011 for review). Interestingly, the K_m value of the type II RubisCO employed in dinoflagellates (80–250 µmol CO₂ l⁻¹) is much higher than the K_m of type I in diatoms (31–41 µmol CO₂ l⁻¹; Badger et al. 1998). In other words, the CCM in these dinoflagellates increased not only their CO₂ affinities by more than one order of magnitude relative to their RubisCO kinetics, but also demonstrates that the activity of the CCM in dinoflagellates must be up to sixfold higher than that of diatoms. Additionally, dinoflagellate cells are typically larger than diatoms, which automatically reduces the surface to volume ratio and hence the specific reaction diffusion-supply rate of CO₂ to the cell surface (Reinfelder 2011). The correspondingly higher energy expenditure for running their CCM could thus, to a large degree, explain why dinoflagellates grow generally much slower than diatoms and thrive under different environmental conditions (Smayda 1997).

Next to the K_{1/2} value, also the maximum rate (V_{max}) plays an important role in determining the competitive success of a species (Healey 1980). Interestingly, our data indicate a trade-off between V_{max} and K_{1/2} values between both species. *Scrippsiella trochoidea* displayed relatively high V_{max} and high K_{1/2} values, while *A. tamarense* showed the inverse pattern, i.e. relatively low V_{max} and low K_{1/2} (Fig. 3). The observed trade-off within the kinetic properties of C_i acquisition is also present between the different CO₂ treatments, especially for *S. trochoidea* showing a relative decrease in affinities with increasing maximum rates. This correlation may reflect fundamental characteristics of nutrient uptake in microalgae (Raven 1980, Aksnes and Egges 1991, Lichtman et al. 2007). Given the limited area of the cell's surface available for nutrient uptake, the number of transporters with small active area per transporter (leading to higher V_{max} and higher K_{1/2}) 'compete' with the number of uptake sites with relatively large active areas (leading to lower V_{max} and lower K_{1/2}).

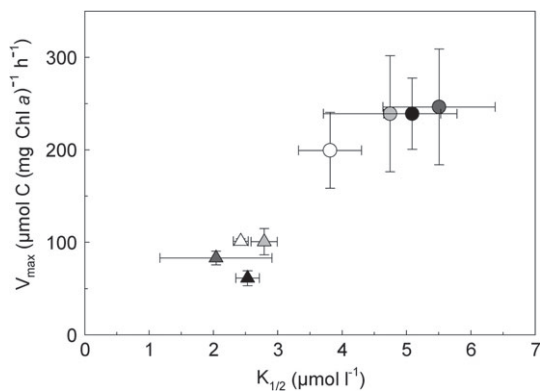


Fig. 3. V_{\max} vs $K_{1/2}$ of photosynthetic carbon fixation of *Scrippsiella trochoidea* (circles), *Alexandrium tamarense* (triangles) acclimated to different CO_2 concentrations. Color of symbols indicates CO_2 treatments from low (white) to high (black). Symbols represent mean \pm SD ($n = 3$).

The fact that cells do not come up with transporters being characterized by high V_{\max} as well as low $K_{1/2}$ is probably dictated by biochemical constraints, i.e. transporters can be faster only at the expense of lower affinities or vice versa (Fersht 1974). Our findings on the trade-off between V_{\max} and $K_{1/2}$ in C_i acquisition are in line with previously observed characteristics on N acquisition in the major eukaryotic phytoplankton groups (Lichtman et al. 2007) as well as different strains of two N_2 fixing cyanobacteria species (Hutchins et al. 2013). However, whether this trade-off in C_i acquisition is a general feature holding true also for other species and strains (Brading et al. 2013 show V_{\max} and $K_{1/2}$ values of two *Symbiodinium* strains being similar to *S. trochoidea*) and even taxa needs to be further investigated.

Ecological implications

To compensate potential limitations in the carboxylation reaction of RubisCO, *S. trochoidea* and *A. tamarense* operate effective CCMs, allowing both species to grow unaltered over the applied range of $p\text{CO}_2$. More specifically, both species substantially increased their overall affinities for photosynthesis, relative to what would be predicted by RubisCO, and were also able to use HCO_3^- as C_i source. However, the high levels of C_i accumulation required for the low affine RubisCO, the predominant HCO_3^- uptake, as well as the high CO_2 leakage cause C_i acquisition to be very costly, which may have profound ecological consequences. For instance, it could partly explain why dinoflagellates display generally lower growth rates compared to other major groups of marine phytoplankton, which employ a more affine type I RubisCO (Smayda 1997). Reasons why dinoflagellates yet thrive well in many environments can

partly be attributed to their mixotrophic behavior (Jeong et al. 2005), the potential of some species to produce allelopathic compounds (Cembella 2003) and the ability to migrate within the water column to circumvent nutrient and light limitation (MacIntyre et al. 1997). Active swimming may as well lower diffusion limitation (Pahlow et al. 1997), in particular for nutrients like nitrate or trace elements, but it could also enhance the CO_2 supply to the cell surface and thereby possibly reduce the costs of CCMs in dinoflagellates.

The observed trade-off between maximum uptake rates and affinities for CO_2 may also play a role in optimizing the competitive success of both species at different CO_2 levels. More specifically, having a higher V_{\max} and higher growth rate, *S. trochoidea* exhibits the 'velocity' strategy (Sommer 1984), which will be favored under high and dynamic C_i availabilities. With a lower $K_{1/2}$, on the other hand, *A. tamarense* exhibits an 'affinity' strategy (Sommer 1984) that will have a competitive advantage under low C_i concentrations (Fig. 3, Table 3). During phytoplankton blooms, carbonate chemistry may substantially change and drift toward high pH and low CO_2 concentrations (Hansen 2002). As a consequence, species with a low $K_{1/2}$ for CO_2 , such as *A. tamarense*, may be favored. At the same time, however, carbonate chemistry may also exhibit strong daily fluctuations as results of day-time photosynthesis and night-time respiration. Under these conditions, species with a high V_{\max} and growth rate, like *S. trochoidea*, are likely to be favored. On top of that, the high preference of *S. trochoidea* for HCO_3^- may further support its growth during blooms. It thus seems that *A. tamarense* and *S. trochoidea* exhibit different strategies allowing them to cope with dense bloom conditions. Such differences in competitive strategies, induced by physiological characteristics, may furthermore allow coexistence of multiple species.

Species being able to regulate their CCM in response toward high $p\text{CO}_2$ and low pH conditions will have advantages in a future ocean. Even though both tested species were regulating their CCM, *S. trochoidea* showed strongest changes in response to OA. Modes of CCMs and thus CO_2 sensitivities in growth and biomass production may, however, change strongly under resource limitation, i.e. nutrient depleted or low light conditions, and therefore alter the outcome of competition under OA. For bloom-forming species like *S. trochoidea* and *A. tamarense*, which tend to flourish late in the succession, investigations on the interactive effects of nutrient limitation and OA as well as dynamic changes therein are crucial to improve our understanding of the response of this important group of phytoplankton in a future, high CO_2 world.

Acknowledgements—Grant support was provided by European Community's Seventh Framework Programme (FP7/2007-2013)/ERC No. 205150, EPOCA No. 211384 and BIOACID programme, financed by the German Ministry of Education and Research. We thank Karin Zonneveld (University of Bremen, Germany) for providing *Scrippsiella trochoidea* strain 267 and Urban Tillmann (Alfred Wegener Institute for Polar and Marine Research, Bremerhaven, Germany) for providing *Alexandrium tamarense* strain Alex5. We thank Klaus-Uwe Richter, Ulrike Richter and Yvette Bublitz for assistance during the work and Sebastian Rokitta for having a critical view on the manuscript.

References

- Aksnes DL, Egge JK (1991) A theoretical model for nutrient uptake in phytoplankton. *Mar Ecol Prog Ser* 70: 65–72
- Amthor JS (1991) Respiration in a future, higher-CO₂ world. *Plant Cell Environ* 14: 13–20
- Badger MR, Price GD (1989) Carbonic anhydrase activity associated with the cyanobacterium *Synechococcus* PCC7942. *Plant Physiol* 89: 51–60
- Badger MR, Palmqvist K, Jian-Wei Y (1994) Measurement of CO₂ and HCO₃⁻ fluxes in cyanobacteria and microalgae during steady-state photosynthesis. *Physiol Plant* 90: 529–536
- Badger MR, Andrews TJ, Whitney SM, Ludwig M, Yellowlees DC, Leggat W, Price GD (1998) The diversity and coevolution of Rubisco, plastids, pyrenoids, and chloroplast-based CO₂-concentrating mechanisms in algae. *Can J Bot* 76: 1052–1071
- Bates HA, Kostriken R, Rapoport H (1978) The occurrence of saxitoxin and other toxins in various dinoflagellates. *Toxicon* 16: 595–601
- Brading P, Warner ME, Davey P, Smith DJ, Achterberg EP, Suggett DJ (2011) Differential effects of ocean acidification on growth and photosynthesis among phylotypes of *Symbiodinium* (Dinophyceae). *Limnol Oceanogr* 56: 927–938
- Brading P, Warner ME, Smith DJ, Suggett DJ (2013) Contrasting modes of inorganic carbon acquisition amongst *Symbiodinium* (Dinophyceae) phylotypes. *New Phytol* 200: 432–442
- Burkhardt S, Zondervan I, Riebesell U (1999) Effect of CO₂ concentration on C:N:P ratio in marine phytoplankton: a species comparison. *Limnol Oceanogr* 44: 683–690
- Burkhardt S, Amoroso S, Riebesell U, Sültemeyer D (2001) CO₂ and HCO₃⁻ uptake in marine diatoms acclimated to different CO₂ concentrations. *Limnol Oceanogr* 46: 1378–1391
- Caldeira K, Wickett ME (2003) Anthropogenic carbon and ocean pH. *Nature* 425: 365
- Carreto JL, Carignan MO, Montoya NG (2001) Comparative studies on mycosporine-like amino acids, paralytic shellfish toxins and pigment profiles of the toxic dinoflagellates *Alexandrium tamarense*, *A. catenella* and *A. minutum*. *Mar Ecol Prog Ser* 223: 49–60
- Cembella AD (2003) Chemical ecology of eukaryotic microalgae in marine ecosystems. *Phycologia* 42: 420–447
- Colman B, Huertas IE, Bhatti S, Dason JS (2002) The diversity of inorganic carbon acquisition mechanisms in eukaryotic microalgae. *Funct Plant Biol* 29: 261–270
- Dason JS, Huertas IE, Colman B (2004) Source of inorganic carbon for photosynthesis in two marine dinoflagellates. *J Phycol* 40: 229–434
- Dickson AG, Millero FJ (1987) A comparison of the equilibrium constants for the dissociation of carbonic acid in seawater media. *Deep-Sea Res* 34: 1733–1743
- Doney SC, Fabry VJ, Feely RA, Kleydas JA (2009) Ocean acidification: the other CO₂ problem. *Annu Rev Mar Sci* 1: 169–192
- Egleston ES, Sabine CL, Morel FMM (2010) Revelle revisited: buffer factors that quantify the response of ocean chemistry to changes in DIC and alkalinity. *Global Biogeochem Cycles* 24: GB1002
- Elzenga JTM, Prins HBA, Stefels J (2000) The role of extracellular carbonic anhydrase activity in inorganic carbon utilization of *Phaeocystis globosa* (Prymnesiophyceae): a comparison with other marine algae using the isotope disequilibrium technique. *Limnol Oceanogr* 45: 372–380
- Fabry JV, Seibel AB, Feely RA, Orr JC (2008) Impacts of ocean acidification on marine fauna and ecosystem processes. *ICES J Mar Sci* 65: 414–432
- Falkowski PG, Barber RT, Smetacek V (1998) Biogeochemical controls and feedbacks on ocean primary production. *Science* 281: 200–206
- Fersht AR (1974) Catalysis, binding and enzyme-substrate complementarity. *Proc R Soc Lond B Biol Sci* 187: 397–407
- Fistarol GO, Legrand C, Rengefors K, Granéli E (2004) Temporary cyst formation in phytoplankton: a response to allelopathic competitors? *Environ Microbiol* 6: 791–798
- Fu FX, Warner ME, Zhang Y, Feng Y, Hutchins DA (2007) Effects of increased temperature and CO₂ on photosynthesis, growth, and elemental ratios in marine *Synechococcus* and *Prochlorococcus* (Cyanobacteria). *J Phycol* 43: 485–496
- Fu FX, Zhang Y, Warner ME, Feng Y, Sun J, Hutchins DA (2008) A comparison of future increased CO₂ and temperature effects on sympatric *Heterosigma akashiwo* and *Prorocentrum minimum*. *Harmful Algae* 7: 76–90
- Fu FX, Place AR, Garcia NS, Hutchins DA (2010) CO₂ and phosphate availability control the toxicity of the harmful bloom dinoflagellate *Karlodinium veneticum*. *Aquat Microb Ecol* 59: 55–56
- Gao K, Xu J, Gao G, Li Y, Hutchins DA, Huang B, Wang L, Zheng Y, Jin P, Cai X, Häder D-P, Li W, Xu K, Liu N,

- Riebesell U (2012) Rising CO₂ and increased light exposure synergistically reduce marine primary productivity. *Nat Clim Change* 2: 519–523
- Giordano M, Beardall J, Raven JA (2005) CO₂ concentrating mechanisms in algae: mechanisms, environmental modulation, and evolution. *Annu Rev Plant Biol* 56: 99–131
- Guillard RRL, Ryther JH (1962) Studies of marine planktonic diatoms: I. *Cyclotella nana* Hustedt, and *Detonula confervacea* Cleve. *Can J Microbiol* 8: 229–239
- Haardt H, Maske H (1987) Specific in vivo absorption coefficient of chlorophyll a at 675 nm. *Limnol Oceanogr* 32: 608–619
- Hansen PJ (2002) Effect of high pH on the growth and survival of marine phytoplankton: implications for species succession. *Aquat Microb Ecol* 28: 279–288
- Healey FP (1980) Slope of the Monod equation as an indicator of advantage in nutrient competition. *Microb Ecol* 5: 281–286
- Hopkinson BM, Meile C, Chen S (2013) Quantification of extracellular carbonic anhydrase activity in two marine diatoms and investigation of its role. *Plant Physiol* 162: 1142–1152
- Hu H, Shi Y, Cong W (2006) Improvement in growth and toxin production of *Alexandrium tamarense* by two-step culture method. *J Appl Phycol* 18: 119–126
- Hutchins DA, Fei-Xue F, Webb EA, Walworth N, Tagliabue A (2013) Taxon-specific response of marine nitrogen fixers to elevated carbon dioxide concentrations. *Nat Geosci* 6: 790–795
- IPCC (2007) Global Climate Projections. In: Solomon S, Qin D, Manning M, Chen Z, Marquis M, Averyt KB, Tignor M, Miller HL (eds) *Climate Change 2007: The Physical Science Basis. Contribution of Working Group I to the Fourth Assessment Report of the Intergovernmental Panel on Climate Change*. Cambridge University Press, Cambridge; New York
- Jeong HJ, Yoo YD, Park JY, Song JY, Kim ST, Lee SH, Kim KY, Yih WH (2005) Feeding by phototrophic red-tide dinoflagellates: five species newly revealed and six species previously known to be mixotrophic. *Aquat Microb Ecol* 40: 133–150
- Knap A, Michaelis A, Close A, Ducklow H, Dickson A (eds) (1996) *Protocols for the Joint Global Ocean Flux Study (JGOFS) Core Measurements*. JGOFS Report No. 19, vi+170 pp. Reprint of the IOC Manuals and Guides No. 29, UNESCO 1994
- Kranz SA, Sültemeyer D, Richter K-U, Rost B (2009) Carbon acquisition by *Trichodesmium*: the effect of pCO₂ and diurnal changes. *Limnol Oceanogr* 54: 548–559
- Lapointe M, MacKenzie TBD, Morse D (2008) An external δ-carbonic anhydrase in a free-living marine dinoflagellate may circumvent diffusion-limited carbon acquisition. *Plant Physiol* 147: 1427–1436
- Leong SCY, Maekawa M, Taguchi S (2010) Carbon and nitrogen acquisition by the toxic dinoflagellate *Alexandrium tamarense* in response to different nitrogen sources and supply modes. *Harmful Algae* 9: 48–58
- Li G, Campbell DA (2013) Rising CO₂ interacts with growth light and growth rate to alter photosystem II photoinactivation of the coastal diatom *Thalassiosira pseudonana*. *PLoS ONE* 8: e55562
- Lichtman E, Klausmeier CA, Schofield OM, Falkowski PG (2007) The role of functional traits and trade-offs in structuring phytoplankton communities: scaling from cellular to ecosystem level. *Ecol Lett* 10: 1170–1181
- MacIntyre JG, Cullen JJ, Cembella AD (1997) Vertical migration, nutrition and toxicity in the dinoflagellate *Alexandrium tamarense*. *Mar Ecol Prog Ser* 148: 201–216
- Martin CL, Tortell PD (2008) Bicarbonate transport and extracellular carbonic anhydrase in marine diatoms. *Physiol Plant* 133: 106–116
- McCollin T, Lichtman D, Bresnan E, Berx B (2011) A study of phytoplankton communities along a hydrographic transect on the north east coast of Scotland. *Marine Scotland Science Report* 04/11
- Mehrbach C, Culbertson CH, Hawley JE, Pytkowicz RM (1973) Measurement of the apparent dissociation constants of carbonic acid in seawater at atmospheric pressure. *Limnol Oceanogr* 18: 897–907
- Morse D, Salois P, Markovic P, Hastings JW (1995) A nuclear-encoded form II RuBisCO in dinoflagellates. *Science* 268: 1622–1624
- Pahlow M, Riebesell U, Wolf-Gladrow DA (1997) Impact of cell shape and chain formation on nutrient acquisition by marine diatoms. *Limnol Oceanogr* 42: 1660–1672
- Palmqvist K, Yu J-W, Badger MR (1994) Carbonic anhydrase activity and inorganic carbon fluxes in low- and high-C_i cells of *Clamydomonas reinhardtii* and *Scenedesmus obliquus*. *Physiol Plant* 90: 537–547
- Pierrot DE, Lewis E, Wallace DWR (2006) Program Developed for CO₂ System Calculations. Carbon Dioxide Information Analysis Center, Oak Ridge National Laboratory. Available at: <http://cdiac.ornl.gov/oceans/co2rprt.html> (accessed 1 March 1997)
- Quinn GP, Keough MJ (2002) *Experimental Design and Data Analysis for Biologists*. Cambridge University Press, Cambridge
- Ratti S, Giordano M (2007) CO₂-concentrating mechanisms of the potentially toxic dinoflagellate *Protoceratium reticulatum* (Dinophyceae, Gonyaulacales). *J Phycol* 43: 693–701
- Raven JA (1980) Nutrient transport in microalgae. *Adv Microb Physiol* 21: 47–226

- Reinfelder JR (2011) Carbon concentrating mechanisms in eukaryotic marine phytoplankton. *Annu Rev Mar Sci* 3: 291–315
- Rokitta SD, Rost B (2012) Effects of CO₂ and their modulation by light in the life-cycle stages of the coccolithophore *Emiliania huxleyi*. *Limnol Oceanogr* 57: 607–618
- Rost B, Riebesell U, Burkhardt S, Sültemeyer D (2003) Carbon acquisition of bloom-forming marine phytoplankton. *Limnol Oceanogr* 48: 55–67
- Rost B, Richter K-U, Riebesell U, Hansen PJ (2006) Inorganic carbon acquisition in red tide dinoflagellates. *Plant Cell Environ* 29: 810–822
- Rost B, Kranz S, Richter K-U, Tortell P (2007) Isotope disequilibrium and mass spectrometric studies of inorganic carbon acquisition by phytoplankton. *Limnol Oceanogr Methods* 5: 328–337
- Rost B, Zondervan I, Wolf-Gladrow DA (2008) Sensitivity of phytoplankton to future changes in ocean carbonate chemistry: current knowledge, contradictions and research directions. *Mar Ecol Prog Ser* 373: 227–237
- Silverman DN (1982) Carbonic anhydrase. Oxygen-18 exchange catalyzed by an enzyme with rate-contributing proton-transfer steps. *Methods Enzymol* 87: 732–752
- Smayda TJ (1997) Harmful algal blooms: their ecophysiology and general relevance to phytoplankton blooms in the sea. *Limnol Oceanogr* 42: 1137–1153
- Sommer U (1984) The paradox of the plankton: fluctuations of phosphorus availability maintain diversity of phytoplankton in flow-through cultures. *Limnol Oceanogr* 29: 633–636
- Sültemeyer D (1998) Carbonic anhydrase in eukaryotic algae: characterization, regulation, and possible function during photosynthesis. *Can J Bot* 76: 962–972
- Tillmann U, Alpermann TL, da Purificação RC, Krock B, Cembella A (2009) Intra-population clonal variability in allelochemical potency of the toxigenic dinoflagellate *Alexandrium tamarense*. *Harmful Algae* 8: 759–769
- Trimborn S, Lundholm N, Thoms S, Richter K-U, Krock B, Hansen PJ, Rost B (2008) Inorganic carbon acquisition in potentially toxic and non-toxic diatoms: the effect of pH-induced changes in seawater carbonate chemistry. *Physiol Plant* 133: 92–105
- Trimborn S, Wolf-Gladrow DA, Richter K-U, Rost B (2009) The effect of pCO₂ on carbon acquisition and intracellular assimilation in four marine diatoms. *J Exp Mar Biol Ecol* 376: 26–36
- Trimborn S, Brenneis T, Sweet E, Rost B (2013) Sensitivity of Antarctic phytoplankton species to ocean acidification: growth, carbon acquisition, and species interaction. *Limnol Oceanogr* 58: 997–1007
- Van de Waal DB, John U, Ziveri P, Reichart G-J, Hoins M, Sluijs A, Rost B (2013) Ocean acidification reduces growth and calcification in a marine dinoflagellate. *PLoS ONE* 8: e65987
- Van de Waal DB, Eberlein T, John U, Wohlrab S, Rost B (2014) Impact of elevated pCO₂ on paralytic shellfish poisoning toxin content and composition in *Alexandrium tamarense*. *Toxicon* 78: 58–67
- Wang ZH, Qi YZ, Yang YF (2007) Cyst formation: an important mechanism for the termination of *Scrippsiella trochoidea* (Dinophyceae) bloom. *J Plankton Res* 29: 209–218
- Williams PJL, Robertson JE (1991) Overall planktonic oxygen and carbon dioxide metabolisms: the problem of reconciling observations and calculations of photosynthetic quotients. *J Plankton Res* 13: 153–169
- Wolf-Gladrow DA, Riebesell U, Burkhardt S, Bijma J (1999) Direct effects of CO₂ concentration on growth and isotopic composition of marine plankton. *Tellus B* 51: 461–476
- Yang G, Gao K (2012) Physiological responses of the marine diatom *Thalassiosira pseudonana* to increased pCO₂ and seawater acidity. *Mar Environ Res* 79: 142–151